
Extending Kernel Trick to Influence Functions

Zhenhuan Sun
University of Toronto
zhsun@ece.utoronto.ca

Shahrokh Valaee
University of Toronto
valaee@ece.utoronto.ca

Abstract

In this paper, we present a dual representation of the influence functions, whose computational complexity scales with dataset size rather than model size. Both analytically and experimentally, we show that this representation can be an efficient alternative to the original influence functions for estimating changes in parameters, model outputs and loss due to data point removal, when model size is large relative to dataset size, or when evaluating the original influence functions in parameter space is infeasible. The dual representation, however, is limited to linearizable models, which are models whose behavior can be approximated by their linearizations throughout training, and requires materializing a matrix, whose size grows with the product of model output dimension and dataset size.

1 Introduction

Interpretability and privacy are critical considerations in many machine learning applications. However, many modern machine learning models, particularly deep neural networks, lack transparency and may inadvertently memorize undesired information or expose sensitive information to users. This creates challenges for understanding model behavior, and raises concerns about the reliability of model predictions and the risk of exposing private information. As a result, there is growing interest in developing methods that improve interpretability and provide mechanisms that remove the influence of sensitive or undesirable information from trained models.

Influence functions, originally developed in robust statistics and later introduced to machine learning by Koh and Liang [1], aim to address these issues by providing a way of estimating how model parameters and parameter-dependent functions change when training data points are perturbed. Due to this ability, influence functions have played a particularly prominent role in machine unlearning [2], which is an emerging field that aims to efficiently remove the influence of specific data points from a trained model so that the resulting model behaves as if it had been retrained from scratch without those data points. Despite being successfully applied to the unlearning of small models [3], influence function based unlearning methods cannot be readily scaled to large models due to the need to compute an inverse Hessian–vector product (IHVP), whose computational complexity grows with the number of model parameters and the cost of evaluating model.

Inspired by the dual formulation of linear regression, in this work, we introduce a dual representation of the influence functions for linearizable models, which shifts the computational complexity of IHVP from scaling with model size to scaling with dataset size. We show that the dual representation can be a more efficient alternative to the original representation when model size is large relative to dataset size, and that it provides a means of estimating changes in model outputs and loss due to data point removal for neural networks with infinitely many parameters.

2 Preliminaries

This section introduces our notations and provides conceptual background needed for the development of the dual representation of influence functions. The derivations of the results in this section are provided in Appendix B.

Let $\mathcal{D} \subseteq \mathcal{X} \times \mathcal{Y}$ be a training dataset of input-output pairs (\mathbf{x}, \mathbf{y}) , where $\mathcal{X} \subseteq \mathbb{R}^{d_{\text{in}}}$ and $\mathcal{Y} \subseteq \mathbb{R}^{d_{\text{out}}}$ denote input and output spaces. We represent \mathcal{D} compactly by the feature matrix $\mathbf{X} \in \mathbb{R}^{|\mathcal{D}| \times d_{\text{in}}}$ and the target matrix $\mathbf{Y} \in \mathbb{R}^{|\mathcal{D}| \times d_{\text{out}}}$. Let $f : \mathbb{R}^{d_{\text{in}}} \times \mathbb{R}^{d_{\theta}} \rightarrow \mathbb{R}^{d_{\text{out}}}$ be a parameterized machine learning model, and consider the regularized empirical risk over \mathcal{D}

$$\mathcal{L}_{\mathcal{D}}(\boldsymbol{\theta}) := \frac{1}{|\mathcal{D}|} \sum_{(\mathbf{x}, \mathbf{y}) \in \mathcal{D}} \left(\ell(f(\mathbf{x}, \boldsymbol{\theta}), \mathbf{y}) + \frac{\lambda}{2} \|\boldsymbol{\theta}\|_2^2 \right),$$

where $\lambda > 0$ denotes a regularization constant and $\ell : \mathbb{R}^{d_{\text{out}}} \times \mathbb{R}^{d_{\text{out}}} \rightarrow \mathbb{R}_{\geq 0}$ denotes a loss function. When ℓ is convex in $\boldsymbol{\theta}$, $\mathcal{L}_{\mathcal{D}}(\boldsymbol{\theta})$ is strictly convex and has a unique minimizer $\boldsymbol{\theta}^* := \arg \min_{\boldsymbol{\theta} \in \mathbb{R}^{d_{\theta}}} \mathcal{L}_{\mathcal{D}}(\boldsymbol{\theta})$ for any dataset \mathcal{D} . We denote the gradients of such empirical risk with respect to parameters and vectorized model outputs at all data points in \mathcal{D} as $\nabla_{\boldsymbol{\theta}} \mathcal{L}_{\mathcal{D}}(\boldsymbol{\theta})$ and $\nabla_{f(\mathbf{X}, \boldsymbol{\theta})} \mathcal{L}_{\mathcal{D}}$, respectively, where $f(\mathbf{X}, \boldsymbol{\theta}) := \text{vec}(\{f(\mathbf{x}, \boldsymbol{\theta})\}_{\mathbf{x} \in \mathcal{D}}) \in \mathbb{R}^{d_{\text{out}}|\mathcal{D}|}$.

2.1 Influence Functions

Let \mathcal{D}_f denote a forget dataset, which contains data points that need to be deleted from \mathcal{D} and whose influence must be removed from $\boldsymbol{\theta}^*$. The remaining data points form a retain dataset, which is denoted as \mathcal{D}_r . Assume, without loss of generality, that data points in \mathcal{D}_f are the first $|\mathcal{D}_f|$ data points in \mathcal{D} . Consider an upweighted version of $\mathcal{L}_{\mathcal{D}}(\boldsymbol{\theta})$, defined as $\mathcal{L}_{\mathcal{D}}(\boldsymbol{\theta}, \epsilon) := \mathcal{L}_{\mathcal{D}}(\boldsymbol{\theta}) + |\mathcal{D}_f| \mathcal{L}_{\mathcal{D}_f}(\boldsymbol{\theta}) \epsilon$, where the contributions of the data points in \mathcal{D}_f are upweighted by ϵ . $\mathcal{L}_{\mathcal{D}}(\boldsymbol{\theta}, \epsilon)$ remains strictly convex and has a unique minimizer $\boldsymbol{\theta}^*(\epsilon) := \arg \min_{\boldsymbol{\theta} \in \mathbb{R}^{d_{\theta}}} \mathcal{L}_{\mathcal{D}}(\boldsymbol{\theta}, \epsilon)$ that satisfies the first-order necessary condition $\nabla_{\boldsymbol{\theta}} \mathcal{L}_{\mathcal{D}}(\boldsymbol{\theta}^*(\epsilon), \epsilon) = 0$ for optimality.

The idea of influence functions is that, instead of solving $\boldsymbol{\theta}_r^* := \arg \min_{\boldsymbol{\theta} \in \mathbb{R}^{d_{\theta}}} \mathcal{L}_{\mathcal{D}_r}(\boldsymbol{\theta})$ from scratch, one can use the first-order necessary condition for optimality and the first-order Taylor expansion of $\nabla_{\boldsymbol{\theta}} \mathcal{L}_{\mathcal{D}}(\boldsymbol{\theta}^*(\epsilon), \epsilon)$ around $\boldsymbol{\theta}^*$ to obtain an approximation of $\boldsymbol{\theta}^*(\epsilon)$,

$$\boldsymbol{\theta}^*(\epsilon) \approx \boldsymbol{\theta}^* - \nabla_{\boldsymbol{\theta}}^2 \mathcal{L}_{\mathcal{D}}(\boldsymbol{\theta}^*, \epsilon)^{-1} \nabla_{\boldsymbol{\theta}} \mathcal{L}_{\mathcal{D}}(\boldsymbol{\theta}^*, \epsilon),$$

and with the relation $\boldsymbol{\theta}_r^* = \boldsymbol{\theta}^*(-\frac{1}{|\mathcal{D}_f|})$, $\boldsymbol{\theta}_r^*$ can be approximated by

$$\boldsymbol{\theta}_r^* \approx \boldsymbol{\theta}^* + \frac{|\mathcal{D}_f|}{|\mathcal{D}|} \mathbf{H}_{\boldsymbol{\theta}^*}^{-1} \nabla_{\boldsymbol{\theta}} \mathcal{L}_{\mathcal{D}_f}(\boldsymbol{\theta}^*), \quad (1)$$

where $\mathbf{H}_{\boldsymbol{\theta}^*} := \nabla_{\boldsymbol{\theta}}^2 \mathcal{L}_{\mathcal{D}}(\boldsymbol{\theta}^*, -\frac{1}{|\mathcal{D}_f|}) \in \mathbb{R}^{d_{\theta} \times d_{\theta}}$ is the Hessian of the upweighted empirical risk, and $\mathbf{H}_{\boldsymbol{\theta}^*}^{-1}$ may be further approximated by $\nabla_{\boldsymbol{\theta}}^2 \mathcal{L}_{\mathcal{D}}(\boldsymbol{\theta}^*)^{-1}$ when $\frac{|\mathcal{D}_f|}{|\mathcal{D}|}$ is small. In addition, for any differentiable function $g : \mathbb{R}^{d_{\theta}} \rightarrow \mathbb{R}^k$, $g(\boldsymbol{\theta}_r^*)$ can be approximated by evaluating the first-order Taylor expansion of $g(\boldsymbol{\theta})$ around $\boldsymbol{\theta}^*$ at $\boldsymbol{\theta}_r^*$. For example, let $\mathbf{z}_t := (\mathbf{x}_t, \mathbf{y}_t)$ denote a test data point, the change in model output and loss at \mathbf{z}_t caused by removing \mathcal{D}_f can be approximated by

$$f(\mathbf{x}_t, \boldsymbol{\theta}_r^*) - f(\mathbf{x}_t, \boldsymbol{\theta}^*) \approx \nabla_{\boldsymbol{\theta}} f(\mathbf{x}_t, \boldsymbol{\theta}^*) (\boldsymbol{\theta}_r^* - \boldsymbol{\theta}^*) \quad (2)$$

$$\mathcal{L}_{\{\mathbf{z}_t\}}(\boldsymbol{\theta}_r^*) - \mathcal{L}_{\{\mathbf{z}_t\}}(\boldsymbol{\theta}^*) \approx \nabla_{\boldsymbol{\theta}} \mathcal{L}_{\{\mathbf{z}_t\}}(\boldsymbol{\theta}^*)^{\top} (\boldsymbol{\theta}_r^* - \boldsymbol{\theta}^*), \quad (3)$$

where $\boldsymbol{\theta}_r^* - \boldsymbol{\theta}^*$ is given by Equation 1.

The computational bottleneck of Equation 1 is the IHVP: $\mathbf{H}_{\boldsymbol{\theta}^*}^{-1} \nabla_{\boldsymbol{\theta}} \mathcal{L}_{\mathcal{D}_f}(\boldsymbol{\theta}^*)$. Since $\mathbf{H}_{\boldsymbol{\theta}^*}$ scales with model size, materializing it and computing its inverse is expensive for large models. Consequently, the IHVP is typically computed using iterative methods such as conjugate gradients (CG), which solve the linear system

$$\mathbf{H}_{\boldsymbol{\theta}^*} \mathbf{s} = \frac{|\mathcal{D}_f|}{|\mathcal{D}|} \nabla_{\boldsymbol{\theta}} \mathcal{L}_{\mathcal{D}_f}(\boldsymbol{\theta}^*) \quad (4)$$

relying solely on a linear operator $\mathbf{x} \mapsto \mathbf{H}_{\boldsymbol{\theta}^*} \mathbf{x}$ that computes Hessian–vector products (HVPs) via automatic differentiation, without materializing the Hessian matrix. Once $\boldsymbol{\theta}_r^*$ is obtained, Equations 2 and 3 can be evaluated by computing the Jacobian–vector products (JVPs) via automatic differentiation, and evaluations at multiple test data points can be parallelized across GPUs.

3 Methodology

This section derives the dual representation of influence functions for linearized models, and discusses the advantages of the dual representation. The proofs and derivations of the results in this section are provided in Appendices A and B.

3.1 Dual Representation

Consider the linearization of $f(\cdot, \boldsymbol{\theta})$ around $\boldsymbol{\theta}'$, defined as $f^{\text{lin}}(\cdot, \boldsymbol{\theta}) := f(\cdot, \boldsymbol{\theta}') + \nabla_{\boldsymbol{\theta}} f(\cdot, \boldsymbol{\theta}')(\boldsymbol{\theta} - \boldsymbol{\theta}')$, and suppose it is trained by minimizing the regularized empirical risk

$$\hat{\mathcal{L}}_{\mathcal{D}}(\boldsymbol{\theta}) := \frac{1}{|\mathcal{D}|} \sum_{(\mathbf{x}, \mathbf{y}) \in \mathcal{D}} \left(\ell(f^{\text{lin}}(\mathbf{x}, \boldsymbol{\theta}), \mathbf{y}) + \frac{\lambda}{2} \|\boldsymbol{\theta} - \boldsymbol{\theta}'\|_2^2 \right).$$

Under this risk, the difference between the parameters obtained by training on any nonempty subset of \mathcal{D} and those obtained by training on \mathcal{D} lies in a linear subspace of $\mathbb{R}^{d_{\boldsymbol{\theta}}}$. This observation is formalized in the following proposition.

Proposition 3.1. *For any nonempty $\mathcal{D}_r \subseteq \mathcal{D}$, let $\hat{\boldsymbol{\theta}}^*$ and $\hat{\boldsymbol{\theta}}_{r,c}^*$ denote the model parameters obtained by solving $\arg \min_{\boldsymbol{\theta} \in \mathbb{R}^{d_{\boldsymbol{\theta}}}} \hat{\mathcal{L}}_{\mathcal{D}}(\boldsymbol{\theta})$ and $\arg \min_{\boldsymbol{\theta} \in \mathbb{R}^{d_{\boldsymbol{\theta}}}} \hat{\mathcal{L}}_{\mathcal{D}_r}(\boldsymbol{\theta})$, respectively. Then:*

$$\hat{\boldsymbol{\theta}}_{r,c}^* - \hat{\boldsymbol{\theta}}^* = \nabla_{\boldsymbol{\theta}} f(\mathbf{X}, \boldsymbol{\theta}')^{\top} \Delta \boldsymbol{\alpha}_r^*,$$

where $\nabla_{\boldsymbol{\theta}} f(\mathbf{X}, \boldsymbol{\theta}') \in \mathbb{R}^{d_{\text{out}}|\mathcal{D}| \times d_{\boldsymbol{\theta}}}$ and $\Delta \boldsymbol{\alpha}_r^* \in \mathbb{R}^{d_{\text{out}}|\mathcal{D}|}$ are defined as

$$\nabla_{\boldsymbol{\theta}} f(\mathbf{X}, \boldsymbol{\theta}') := \begin{bmatrix} \nabla_{\boldsymbol{\theta}} f(\mathbf{x}^{(1)}, \boldsymbol{\theta}') \\ \vdots \\ \nabla_{\boldsymbol{\theta}} f(\mathbf{x}^{(|\mathcal{D}|)}, \boldsymbol{\theta}') \end{bmatrix} \quad \Delta \boldsymbol{\alpha}_r^* := \begin{bmatrix} \frac{1}{\lambda} \nabla_{f^{\text{lin}}}(\mathbf{x}_f, \hat{\boldsymbol{\theta}}^*) \hat{\mathcal{L}}_{\mathcal{D}} \\ -\frac{1}{\lambda} \left(\nabla_{f^{\text{lin}}}(\mathbf{x}_r, \hat{\boldsymbol{\theta}}_{r,c}^*) \hat{\mathcal{L}}_{\mathcal{D}_r} - \nabla_{f^{\text{lin}}}(\mathbf{x}_r, \hat{\boldsymbol{\theta}}^*) \hat{\mathcal{L}}_{\mathcal{D}} \right) \end{bmatrix}.$$

Proposition 3.1 implies that, for every nonempty $\mathcal{D}_r \subseteq \mathcal{D}$, the solution to $\arg \min_{\boldsymbol{\theta} \in \mathbb{R}^{d_{\boldsymbol{\theta}}}} \hat{\mathcal{L}}_{\mathcal{D}_r}(\boldsymbol{\theta})$ always belongs to the convex subspace $\mathcal{C} := \hat{\boldsymbol{\theta}}^* + \text{col}(\nabla_{\boldsymbol{\theta}} f(\mathbf{X}, \boldsymbol{\theta}')^{\top})$ of $\mathbb{R}^{d_{\boldsymbol{\theta}}}$, where $\text{col}(A)$ denotes the column space of A . Therefore, the original unconstrained problem can be reformulated as a constrained one, and the following proposition shows that the two problems are equivalent in the sense that they yield the same unique minimizer.

Proposition 3.2. *Assume ℓ is convex with respect to model output, then for any nonempty $\mathcal{D}_r \subseteq \mathcal{D}$, $\arg \min_{\boldsymbol{\theta} \in \mathcal{C}} \hat{\mathcal{L}}_{\mathcal{D}_r}(\boldsymbol{\theta})$ and $\arg \min_{\boldsymbol{\theta} \in \mathbb{R}^{d_{\boldsymbol{\theta}}}} \hat{\mathcal{L}}_{\mathcal{D}_r}(\boldsymbol{\theta})$ have the same unique minimizer.*

To solve the constrained problem, one can introduce a reparameterization that enforces the constraint, and reformulates the problem as an unconstrained one. We enforce the constraint $\boldsymbol{\theta} \in \mathcal{C}$ via the reparameterization

$$\boldsymbol{\theta} := \phi(\Delta \boldsymbol{\alpha}) := \hat{\boldsymbol{\theta}}^* + \nabla_{\boldsymbol{\theta}} f(\mathbf{X}, \boldsymbol{\theta}')^{\top} \Delta \boldsymbol{\alpha},$$

where $\Delta \boldsymbol{\alpha} \in \mathbb{R}^{d_{\text{out}}|\mathcal{D}|}$. Under the reparameterization, $f^{\text{lin}}(\cdot, \boldsymbol{\theta})$ becomes $g^{\text{lin}}(\cdot, \Delta \boldsymbol{\alpha}) := f^{\text{lin}}(\cdot, \hat{\boldsymbol{\theta}}^*) + \mathbf{K}(\cdot, \mathbf{X}) \Delta \boldsymbol{\alpha}$ and $\hat{\mathcal{L}}_{\mathcal{D}}(\boldsymbol{\theta})$ becomes

$$\tilde{\mathcal{L}}_{\mathcal{D}}(\Delta \boldsymbol{\alpha}) := \frac{1}{|\mathcal{D}|} \sum_{(\mathbf{x}, \mathbf{y}) \in \mathcal{D}} \left(\ell(g^{\text{lin}}(\mathbf{x}, \Delta \boldsymbol{\alpha}), \mathbf{y}) + \frac{\lambda}{2} \|\phi(\Delta \boldsymbol{\alpha}) - \boldsymbol{\theta}'\|_2^2 \right),$$

where $\mathbf{K}(\cdot, \cdot) := \nabla_{\boldsymbol{\theta}} f(\cdot, \boldsymbol{\theta}') \nabla_{\boldsymbol{\theta}} f(\cdot, \boldsymbol{\theta}')^{\top}$ denotes the empirical Neural Tangent Kernel (NTK) [4], and $\mathbf{K}(\mathbf{X}_1, \mathbf{X}_2) \in \mathbb{R}^{d_{\text{out}}N_1 \times d_{\text{out}}N_2}$ for feature matrices $\mathbf{X}_1 \in \mathbb{R}^{N_1 \times d_{\text{in}}}$ and $\mathbf{X}_2 \in \mathbb{R}^{N_2 \times d_{\text{in}}}$. $\tilde{\mathcal{L}}_{\mathcal{D}}(\Delta \boldsymbol{\alpha})$ is a dual representation of $\hat{\mathcal{L}}_{\mathcal{D}}(\boldsymbol{\theta})$ and an unconstrained formulation of the constrained problem. The relationship between the solutions to the unconstrained problem in $\Delta \boldsymbol{\alpha}$ and the constrained problem in $\boldsymbol{\theta}$ is stated in the following proposition.

Proposition 3.3. *If ℓ is convex with respect to model output, $\lambda > 0$, and $\nabla_{\boldsymbol{\theta}} f(\mathbf{X}, \boldsymbol{\theta}')$ has full row rank, then for any nonempty $\mathcal{D}_r \subseteq \mathcal{D}$, $\arg \min_{\Delta \boldsymbol{\alpha} \in \mathbb{R}^{d_{\text{out}}|\mathcal{D}|}} \tilde{\mathcal{L}}_{\mathcal{D}_r}(\Delta \boldsymbol{\alpha})$ and $\arg \min_{\boldsymbol{\theta} \in \mathcal{C}} \hat{\mathcal{L}}_{\mathcal{D}_r}(\boldsymbol{\theta})$ have unique minimizers $\Delta \boldsymbol{\alpha}_r^*$ and $\hat{\boldsymbol{\theta}}_{r,c}^*$ that are related by $\Delta \boldsymbol{\alpha}_r^* \xrightarrow[\phi^{-1}(\cdot)]{\phi(\cdot)} \hat{\boldsymbol{\theta}}_{r,c}^*$.*

Proposition 3.2 and 3.3 together imply that, for linearized models and any nonempty $\mathcal{D}_r \subseteq \mathcal{D}$, solving $\arg \min_{\Delta \boldsymbol{\alpha} \in \mathbb{R}^{d_{\text{out}}|\mathcal{D}|}} \tilde{\mathcal{L}}_{\mathcal{D}_r}(\Delta \boldsymbol{\alpha})$ is equivalent to solving $\arg \min_{\boldsymbol{\theta} \in \mathbb{R}^{d_{\boldsymbol{\theta}}}} \hat{\mathcal{L}}_{\mathcal{D}_r}(\boldsymbol{\theta})$, in the sense that both lead to the same parameter $\hat{\boldsymbol{\theta}}_{r,c}^* := \arg \min_{\boldsymbol{\theta} \in \mathcal{C}} \hat{\mathcal{L}}_{\mathcal{D}_r}(\boldsymbol{\theta})$ and the same empirical risk $\hat{\mathcal{L}}_{\mathcal{D}_r}(\hat{\boldsymbol{\theta}}_{r,c}^*)$.

3.2 Influence on $\Delta\alpha$

The dual representation of $\hat{\mathcal{L}}_{\mathcal{D}}(\theta)$ provides an alternative way to obtain $\hat{\theta}^*$. Specifically, $\hat{\theta}^*$ can be obtained by first obtaining $\Delta\alpha^* = \arg \min_{\Delta\alpha \in \mathbb{R}^{d_{\text{out}}|\mathcal{D}|}} \tilde{\mathcal{L}}_{\mathcal{D}}(\Delta\alpha)$, then mapping $\Delta\alpha^*$ back to $\hat{\theta}^*$ via $\phi(\cdot)$. Therefore, to study the influence of removing a subset of data points from \mathcal{D} on $\hat{\theta}^*$, it suffices to study the influence on $\Delta\alpha^*$. For any nonempty $\mathcal{D}_r \subseteq \mathcal{D}$, define $\Delta\alpha_r^* := \arg \min_{\Delta\alpha \in \mathbb{R}^{d_{\text{out}}|\mathcal{D}|}} \tilde{\mathcal{L}}_{\mathcal{D}_r}(\Delta\alpha)$, by following the same derivation as in Section 2.1 and using the fact that $\Delta\alpha^* = \mathbf{0}$, $\Delta\alpha_r^*$ can be approximated by

$$\Delta\alpha_r^* \approx \frac{|\mathcal{D}_f|}{|\mathcal{D}|} \mathbf{H}_{\Delta\alpha^*}^{-1} \nabla_{\Delta\alpha} \tilde{\mathcal{L}}_{\mathcal{D}_f}(\mathbf{0}), \quad (5)$$

where $\mathbf{H}_{\Delta\alpha^*} := \nabla_{\Delta\alpha}^2 \tilde{\mathcal{L}}_{\mathcal{D}}(\mathbf{0}, -\frac{1}{|\mathcal{D}|}) \in \mathbb{R}^{d_{\text{out}}|\mathcal{D}| \times d_{\text{out}}|\mathcal{D}|}$ and $\mathbf{H}_{\Delta\alpha^*}^{-1}$ may be further approximated by $\nabla_{\Delta\alpha}^2 \tilde{\mathcal{L}}_{\mathcal{D}}(\mathbf{0})^{-1}$ when $\frac{|\mathcal{D}_f|}{|\mathcal{D}|}$ is small. Furthermore, Equation 5 can be expressed entirely in terms of the NTK. Let \mathbf{K} , \mathbf{K}_r and \mathbf{K}_f denote $\mathbf{K}(\mathbf{X}, \mathbf{X})$, $\mathbf{K}(\mathbf{X}_r, \mathbf{X})$ and $\mathbf{K}(\mathbf{X}_f, \mathbf{X})$, respectively, $\mathbf{H}_{\Delta\alpha^*}$ and $\nabla_{\Delta\alpha} \tilde{\mathcal{L}}_{\mathcal{D}_f}(\mathbf{0})$ can be expressed as

$$\mathbf{H}_{\Delta\alpha^*} = \frac{|\mathcal{D}_r|}{|\mathcal{D}|} \left(\mathbf{K}_r^\top \nabla_{f^{\text{lin}}(\mathbf{X}_r, \hat{\theta}^*)}^2 \hat{\mathcal{L}}_{\mathcal{D}_r} \mathbf{K}_r + \lambda \mathbf{K} \right) \quad (6)$$

$$\nabla_{\Delta\alpha} \tilde{\mathcal{L}}_{\mathcal{D}_f}(\mathbf{0}) = \mathbf{K}_f^\top \nabla_{f^{\text{lin}}(\mathbf{X}_f, \hat{\theta}^*)} \hat{\mathcal{L}}_{\mathcal{D}_f} + \lambda \mathbf{K} \alpha^*, \quad (7)$$

where $\alpha^* := -\frac{1}{\lambda} \nabla_{f^{\text{lin}}(\mathbf{X}, \hat{\theta}^*)} \hat{\mathcal{L}}_{\mathcal{D}} \in \mathbb{R}^{d_{\text{out}}|\mathcal{D}|}$, and $\nabla_{f^{\text{lin}}(\mathbf{X}_r, \hat{\theta}^*)}^2 \hat{\mathcal{L}}_{\mathcal{D}_r} \in \mathbb{R}^{d_{\text{out}}|\mathcal{D}_r| \times d_{\text{out}}|\mathcal{D}_r|}$ is the Hessian of $\hat{\mathcal{L}}_{\mathcal{D}_r}$ with respect to model outputs, evaluated at $f^{\text{lin}}(\mathbf{X}_r, \hat{\theta}^*) := \text{vec}(\{f^{\text{lin}}(\mathbf{x}, \hat{\theta}^*)\}_{\mathbf{x} \in \mathcal{D}_r}) \in \mathbb{R}^{d_{\text{out}}|\mathcal{D}_r|}$. After obtaining $\Delta\alpha_r^*$, the change in model output and loss at a test data point \mathbf{z}_t can be approximated by the first-order Taylor expansion of $g^{\text{lin}}(\mathbf{x}_t, \Delta\alpha_r^*)$ and $\tilde{\mathcal{L}}_{\{\mathbf{z}_t\}}(\Delta\alpha_r^*)$ around $\mathbf{0}$,

$$f^{\text{lin}}(\mathbf{x}_t, \hat{\theta}_r^*) - f^{\text{lin}}(\mathbf{x}_t, \hat{\theta}^*) \approx \mathbf{K}(\mathbf{x}_t, \mathbf{X}) \Delta\alpha_r^* \quad (8)$$

$$\hat{\mathcal{L}}_{\{\mathbf{z}_t\}}(\hat{\theta}_r^*) - \hat{\mathcal{L}}_{\{\mathbf{z}_t\}}(\hat{\theta}^*) \approx \nabla_{\Delta\alpha} \tilde{\mathcal{L}}_{\{\mathbf{z}_t\}}(\mathbf{0})^\top \Delta\alpha_r^*. \quad (9)$$

3.3 Advantages of working in $\Delta\alpha$ -space

Equation 5, 8, and 9 are the $\Delta\alpha$ -space counterparts of Equation 1, 2 and 3. Although working in the $\Delta\alpha$ -space may appear less convenient due to the additional step of mapping back to the θ -space, it nonetheless offers two advantages over working directly in θ -space.

It can be seen from Proposition 3.1 that, entries of $\Delta\alpha_r^*$ corresponding to data points in \mathcal{D}_f , i.e., $\Delta\alpha_{r,f}^* := \frac{1}{\lambda} \nabla_{f^{\text{lin}}(\mathbf{X}_f, \hat{\theta}^*)} \hat{\mathcal{L}}_{\mathcal{D}}$, are known once $\hat{\theta}^*$ is known. This gives rise to a computational shortcut for evaluating Equation 5. Let \mathbf{K}_{ij} denotes $\mathbf{K}(\mathbf{X}_i, \mathbf{X}_j)$, Equation 5 can be expressed in block matrix form as

$$\begin{bmatrix} \mathbf{H}_{\Delta\alpha^*}^{ff} & \mathbf{H}_{\Delta\alpha^*}^{fr} \\ \mathbf{H}_{\Delta\alpha^*}^{rf} & \mathbf{H}_{\Delta\alpha^*}^{rr} \end{bmatrix} \begin{bmatrix} \Delta\alpha_{r,f}^* \\ \Delta\alpha_{r,r}^* \end{bmatrix} = \frac{|\mathcal{D}_f|}{|\mathcal{D}|} \begin{bmatrix} \nabla_{\Delta\alpha} \tilde{\mathcal{L}}_{\mathcal{D}_f}(\mathbf{0})_f \\ \nabla_{\Delta\alpha} \tilde{\mathcal{L}}_{\mathcal{D}_f}(\mathbf{0})_r \end{bmatrix},$$

where

$$\mathbf{H}_{\Delta\alpha^*}^{ij} = \frac{|\mathcal{D}_r|}{|\mathcal{D}|} \left(\mathbf{K}_{ir} \nabla_{f^{\text{lin}}(\mathbf{X}_r, \hat{\theta}^*)}^2 \hat{\mathcal{L}}_{\mathcal{D}_r} \mathbf{K}_{rj} + \lambda \mathbf{K}_{ij} \right) \quad (10)$$

$$\nabla_{\Delta\alpha} \tilde{\mathcal{L}}_{\mathcal{D}_f}(\mathbf{0})_i = \mathbf{K}_{if} \nabla_{f^{\text{lin}}(\mathbf{X}_f, \hat{\theta}^*)} \hat{\mathcal{L}}_{\mathcal{D}_f} + \lambda \mathbf{K}_i \alpha^*. \quad (11)$$

Since $\Delta\alpha_{r,f}^*$ is known and $\mathbf{H}_{\Delta\alpha^*}^{rr} \in \mathbb{R}^{d_{\text{out}}|\mathcal{D}_r| \times d_{\text{out}}|\mathcal{D}_r|}$ is positive definite when $\mathbf{H}_{\Delta\alpha^*}$ is positive definite, to find $\Delta\alpha_r^*$, it suffices to find $\Delta\alpha_{r,r}^*$ by solving

$$\mathbf{H}_{\Delta\alpha^*}^{rr} \Delta\alpha_{r,r}^* = \frac{|\mathcal{D}_f|}{|\mathcal{D}|} \nabla_{\Delta\alpha} \tilde{\mathcal{L}}_{\mathcal{D}_f}(\mathbf{0})_r - \mathbf{H}_{\Delta\alpha^*}^{rf} \Delta\alpha_{r,f}^*. \quad (12)$$

Linear system 12 has two key properties: (i) the dimension of $\mathbf{H}_{\Delta\alpha^*}^{rr}$ grows with $d_{\text{out}}|\mathcal{D}_r|$ instead of d_θ , and (ii) the size of the system decreases as $|\mathcal{D}_f|$ increases. Therefore, depending on the values of d_{out} and $|\mathcal{D}_f|$, the system can be solved either by forming $\mathbf{H}_{\Delta\alpha^*}^{rr}$ explicitly and using a standard

linear system solver, or by applying CG with an operator that evaluates $\mathbf{H}_{\Delta\alpha^*}^{rr} \mathbf{v}$. In either case, the computational cost of solving the system is independent of model size, and a larger $|\mathcal{D}_f|$ yields a smaller system, reducing the cost even further.

Equations 8 and 9 can be efficiently evaluated at multiple test data points via vectorization. Specifically, let \mathcal{D}_t denote a test dataset, the change in model output at all data points in \mathcal{D}_t can be computed by $\mathbf{K}_t \Delta\alpha^*$, and the change in loss at all data points in \mathcal{D}_t can be computed by

$$|\mathcal{D}_t| \nabla_{f^{\text{lin}}(\mathbf{x}_t, \hat{\theta}^*)} \hat{\mathcal{L}}_{\mathcal{D}_t} \odot (\mathbf{K}_t \Delta\alpha^*) + \lambda \alpha^{*\top} \mathbf{K} \Delta\alpha^* \mathbf{1}, \quad (13)$$

where \mathbf{K}_t denotes $\mathbf{K}(\mathbf{X}_t, \mathbf{X})$ and $\mathbf{1} \in \mathbb{R}^{d_{\text{out}}|\mathcal{D}_t|}$ denotes the all-ones vector¹. Since these two expressions depend on the NTK matrix instead of the Jacobians, being able to evaluate the NTK value between any two data points is sufficient to compute them. Therefore, we can avoid explicitly introducing the NTK features $\nabla_{\theta} f(\mathbf{x}^{(i)}, \theta')$ $\forall i$ and computing the dot products $\nabla_{\theta} f(\mathbf{x}^{(i)}, \theta')^\top \nabla_{\theta} f(\mathbf{x}^{(j)}, \theta')$ $\forall i, j$, and instead evaluate them implicitly through a function. This allows us to compute the influence of removing data points on the loss and model outputs of infinitely wide neural networks whose NTKs admit analytical forms [4, 5].

3.4 Discussion

The estimates provide by influence functions are most reliable when the empirical risk is strictly convex with respect to model parameters, and model is trained to convergence, i.e., $\|\nabla_{\theta} \mathcal{L}_{\mathcal{D}}(\theta^*)\|_2 = 0$. In addition to the conditions stated in Proposition 3.3, the reliable use of the dual representation requires model to be linearizable. Informally, we say a parameterized model is linearizable at some reference point θ' if the model and its linearization around θ' produce similar training dynamics, i.e., parameter updates, predictions, and losses, throughout training. Concretely, this means training $f(\cdot, \theta)$ and $f^{\text{lin}}(\cdot, \theta)$ yields closely aligned parameter trajectories and model output trajectories throughout optimization when the same optimizer is used for both models².

Apart from linear and linearized models, nonlinear models can be made approximately linearizable by training with $\hat{\mathcal{L}}_{\mathcal{D}}$ using large values of λ . This is because a nonlinear model is well approximated by its linearization around θ' when its parameters change little from θ' during training, and the regularization term $\lambda \|\theta - \theta'\|_2^2$ discourages the parameters from deviating too far from θ' when λ is large. Therefore, when trained with large λ , the above results may still hold even if the linearized model $f^{\text{lin}}(\cdot, \theta)$ in $\hat{\mathcal{L}}_{\mathcal{D}}$ is replaced by its nonlinear counterpart $f(\cdot, \theta)$. Moreover, the results in Sections 3.1 and 3.2 can be extended to settings in which $\hat{\mathcal{L}}_{\mathcal{D}}$ is regularized by $\|\theta\|_2^2$. However, in this case, the θ' in $f^{\text{lin}}(\cdot, \theta)$ should be set to $\mathbf{0}$ to ensure consistency with the regularization term. When $f(\cdot, \theta)$ is linear, this gives $f^{\text{lin}}(\cdot, \theta) = f(\cdot, \theta)$.

4 Experiments

This section presents empirical verification of the advantages claimed in Section 3.3 for working in $\Delta\alpha$ -space and investigates how the choice of λ affects the training dynamics of nonlinear models and the effectiveness of the two representations of influence functions. All experiments are implemented in Python using JAX [6] and Neural Tangents [7–11] libraries, and all results are obtained on two NVIDIA RTX 3080 Ti GPUs. The code to reproduce the experiments in this section can be found in https://github.com/ZhenhuanSun/ntk_influence.

4.1 Implementation Details

We assume \mathbf{K} is precomputed and stored, and solve linear system 12 using CG with an operator that evaluates $\mathbf{H}_{\Delta\alpha^*}^{rr} \mathbf{v}$. The operator $\mathbf{v} \mapsto \mathbf{H}_{\Delta\alpha^*}^{rr} \mathbf{v}$ is implemented using Equation 10 as

$$\mathbf{v} \mapsto \frac{|\mathcal{D}_r|}{|\mathcal{D}|} \left(\mathbf{K}_{rr} \left(\nabla_{f^{\text{lin}}(\mathbf{x}_r, \hat{\theta}^*)}^2 \hat{\mathcal{L}}_{\mathcal{D}_r} (\mathbf{K}_{rr} \mathbf{v}) \right) + \lambda \mathbf{K}_{rr} \mathbf{v} \right),$$

¹Equation 13 can be used directly for scalar-valued model, i.e., $d_{\text{out}} = 1$. For vector-valued model, one needs to sum every d_{out} consecutive rows of the first term and change the dimension of $\mathbf{1}$ in the second term to $\mathbb{R}^{|\mathcal{D}_t|}$.

²Assuming all sources of randomness in optimization process, e.g., initialization and mini-batch sampling, are identical.

where \mathbf{K}_{rr} is obtained by slicing \mathbf{K} and our implementation relies on a combination of HVPs and matrix-vector products. In practice, \mathbf{K}_{rr} may be stored either on a single GPU or sharded across multiple GPUs to reduce per-device memory usage. In the latter case, we implement a sharded version of the map $\mathbf{v} \mapsto \mathbf{K}_{rr}\mathbf{v}$ that allows $\mathbf{K}_{rr}\mathbf{v}$ to be evaluated while keeping the shards of \mathbf{K}_{rr} distributed across multiple devices.

4.2 Linearized Models

We verify the computational advantage of the dual representation of influence functions, hereafter referred to as the $\Delta\alpha$ -space method, by comparing its unlearning performance with the original influence functions, hereafter referred to as the θ -space method, on two linearized neural networks and two datasets. For each model-dataset pair, we train the model on full dataset, remove $p \in \{10, 30, 50, 70, 90\}$ percent of the data points randomly from either all classes or a specific class of the dataset, and apply both methods for unlearning. The unlearning performance of both methods is evaluated using the following metrics:

1. **Cold-start runtime**, defined as the time required to run each method on its first execution. This includes not only the time to prepare and solve the linear systems, but also one-time overhead such as compilation, memory allocation, and other initialization costs. This metric compares unlearning speed in scenarios where unlearning is required only once. To accurately measure this runtime, for each value of p , the experiment is run in a separate process to prevent reuse of compiled functions and cached resources;
2. **Warm-start runtime**, defined as the mean and standard deviation of the runtime over five subsequent executions after initialization overhead has been incurred. This metric compares unlearning speed in scenarios where unlearning needs to be performed repeatedly on different \mathcal{D}_f of the same size;
3. **Relative ℓ_2 distance** between the unlearned model parameters θ_u and the retrained model parameters $\hat{\theta}_r^*$, which measures how closely the unlearned model aligns with the retrained model in parameter space. A smaller value indicates better alignment between them;
4. **Accuracy** of the unlearned models and the retrained model on \mathcal{D}_f , which is used to assess forgetting quality. The closer the accuracy of the unlearned model is to that of the retrained model, the stronger the indication that the unlearned model has forgotten the designated data points to a degree similar to the retrained model.

We consider the linearizations of two models: a fully connected neural network (FCNN) with three hidden layers of width 1024 and ReLU activations, and a convolutional neural network (CNN) composed of three blocks, each consisting of a convolutional layer with 128 channels and a 3×3 kernel, followed by a ReLU activation and average pooling. The FCNN and CNN are both linearized around their initialization and trained, respectively, on a subset of MNIST [12] consisting of 200 data points from each of the 10 classes and on a subset of CIFAR-10 [13] consisting of 1000 data points from each of classes 0 (airplane) and 1 (automobile). For FCNN-MNIST pair, training is performed by minimizing $\hat{\mathcal{L}}_{\mathcal{D}}$ with cross entropy loss and $\lambda = 10^{-2}$ using full-batch gradient descent, and data points are randomly removed from all classes of the constructed dataset. For the CNN-CIFAR-10 pair, training is performed by minimizing $\hat{\mathcal{L}}_{\mathcal{D}}$ with squared error loss and $\lambda = 10^{-1}$ using momentum, and data points are removed from class 0 of the constructed dataset. To highlight the effect of unlearning, we include a random perturbation baseline that perturbs the trained model parameter $\hat{\theta}^*$ with random noise $\epsilon \in \mathbb{R}^{d_{\theta}}$, where ϵ satisfies $\|\epsilon\|_2 = \|\hat{\theta}^* - \hat{\theta}_r^*\|_2$. The unlearning performance of the θ -space and $\Delta\alpha$ -space methods on these models is shown in Figure 1.

For both experiments, two implementations of the $\Delta\alpha$ -space method achieve lower runtime than the θ -space method across all percentage of removal. In particular, the sharded implementation has shorter runtime in the cold start scenario, whereas the non-sharded implementation has shorter runtime in the warm start scenario. These results are consistent with our expectations, since the dataset size in both experiments are small relative to the model size, i.e., $d_{\text{out}}|\mathcal{D}| \ll d_{\theta}$. Consequently, the cost of solving linear system 12 is smaller than that of solving linear system 4. In addition, the unlearning performance of the $\Delta\alpha$ -space method is comparable to that of the θ -space method, which can be seen by the small relative ℓ_2 distance between $\hat{\theta}_r^*$ and θ_u produced by both methods and by their close agreement with the retrained model in accuracy on \mathcal{D}_f .

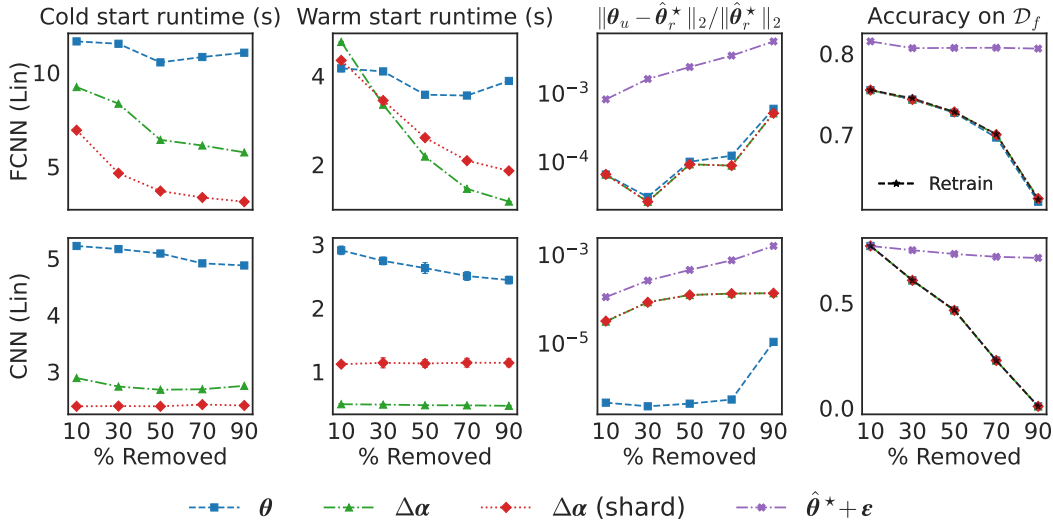


Figure 1: **Comparison of the unlearning performance of θ -space and $\Delta\alpha$ -space methods on linearized FCNN and CNN trained on subsets of MNIST and CIFAR10.** The top and bottom rows correspond to the linearized FCNN and CNN, respectively. We compare the θ -space method with two implementations of the $\Delta\alpha$ -space method, and with a random perturbation baseline. From left to right, we report cold-start runtime, warm-start runtime, relative parameter distance, and test accuracy as a function of the percentage of removed data. The dashed black curves in the rightmost panes indicate the accuracy of the retrained model. We observe that, when model size is large relative to dataset size, the $\Delta\alpha$ -space method requires less runtime while maintaining unlearning performance comparable to that of the θ -space method.

4.3 Effect of λ

To investigate how λ affects the training dynamics of nonlinear models and how these dynamics compare with those of their linearizations, we simultaneously train a nonlinear model and its linearization, using the same loss and optimizer, and record their training dynamics for different values of λ .

We adopt a scalar-valued FCNN with two hidden layers of width 2048 and ReLU activations. Both the model and its linearization around initialization are trained by minimizing $\hat{\mathcal{L}}_{\mathcal{D}}(\theta)$ with squared error loss on a binary MNIST dataset consisting of 5000 data points from each of the classes 3 and 8, using full-batch gradient descent with a learning rate of 0.1. During training, we record the relative ℓ_2 distance between the parameters of the FCNN and its linearization, denoted by θ and θ^{lin} , respectively; the root mean squared error (RMSE) between their predictions on \mathcal{D}_t ; the accuracy performance of both models on \mathcal{D}_t ; and the gradient norms of the parameters of the FCNN and its linearization. These quantities, recorded over 4000 epochs of training, are summarized in Figure 3.

We observe that larger values of λ make the training dynamics of the FCNN more closely resemble that of its linearization, as evidenced by the small relative ℓ_2 distance between their parameters and small difference between their outputs throughout training. In addition, $\|\nabla_{\theta}\mathcal{L}_{\mathcal{D}}(\theta)\|_2$ approaches 0 more rapidly for larger values of λ , indicating that, when trained with $\lambda\|\theta - \theta'\|_2^2$, both the model and its linearization converge faster under stronger regularization. However, this comes at the cost of worse test accuracy, as larger values of λ lead to progressively poorer test accuracy.

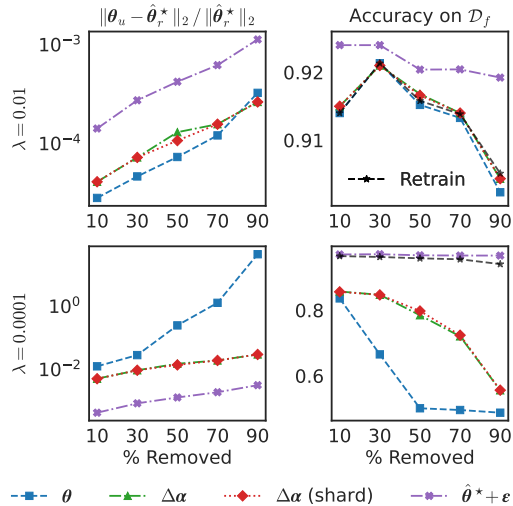


Figure 2: **Comparison of the unlearning performance of θ -space and $\Delta\alpha$ -space methods on a nonlinear model under different values of λ .** The dashed black curves indicate the accuracy of the retrained model.

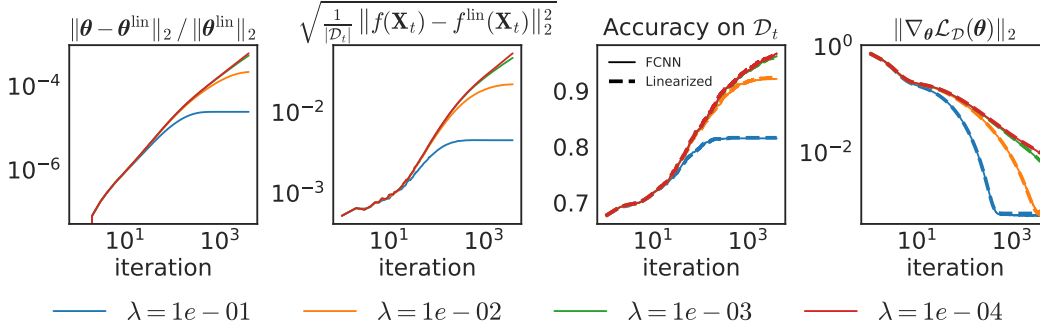


Figure 3: **Comparison of the training dynamics of a FCNN and its linearization under different values of λ .** The left two panes show the relative ℓ_2 distance between the parameters of FCNN and its linearization, and the RMSE between their predictions on \mathcal{D}_t . The right two panes show the accuracies of the FCNN and its linearization on \mathcal{D}_t , and the gradient norms of their parameters. We observe that larger values of λ make the FCNN track its linearization more closely and converge faster, but at the cost of worse test accuracy.

Since the dual representation requires the model to be linearizable, and the original representation also benefits from working with linear models, because they make the empirical risk strictly convex in θ , the choice of λ plays an important role in the effectiveness of θ -space and $\Delta\alpha$ -space methods when they are applied to nonlinear models. This sensitivity to λ is illustrated in Figure 2, where data points from both classes are unlearned from the aforementioned FCNN, trained with different values of λ , using both methods. It can be seen that both methods produce unlearned model that more faithfully match the retrained model, when applied to the FCNN trained with larger value of λ .

4.4 Infinitely Wide Neural Networks

We showcase the applicability of $\Delta\alpha$ -space method to infinitely wide neural networks for estimating changes in model outputs and loss induced by data point removal. We consider two infinitely wide neural networks derived from a FCNN with three hidden layers and ReLU activations, and from a CNN with three convolutional layers and ReLU activations, respectively. The infinitely wide FCNN is trained by minimizing $\hat{\mathcal{L}}_{\mathcal{D}}$ with cross entropy loss and $\lambda = 10^{-1}$ on a subset of MNIST consisting of 1000 data points from each of the 10 classes, whereas the infinitely wide CNN is trained by minimizing $\hat{\mathcal{L}}_{\mathcal{D}}$ with squared error loss and $\lambda = 10^{-1}$ on a subset of CIFAR-10 consisting of 500 data points from each of classes 0 and 1. In both cases, optimization is performed in function space by Kernel Gradient Descent (KGD) [4]

$$f^{(k+1)}(\mathbf{X}) = f^{(k)}(\mathbf{X}) - \eta \cdot \left(\mathbf{K}^{\infty} \nabla_{f^{(k)}(\mathbf{X})} \hat{\mathcal{L}}_{\mathcal{D}} + \lambda \cdot (f^{(k)}(\mathbf{X}) - f^{(0)}(\mathbf{X})) \right), \quad (14)$$

where $f^{(k)}(\mathbf{X}) \in \mathbb{R}^{d_{\text{out}} \times |\mathcal{D}|}$ denotes the outputs of infinitely wide neural network at all training data points at the k -th training iteration, and $\mathbf{K}^{\infty} := \mathbf{K}^{\infty}(\mathbf{X}, \mathbf{X})$ denotes the analytical NTK matrix³. During training, $f^{(0)}(\mathbf{X})$ is initialized to $\mathbf{0}$ and KGD is run for 5000 epochs. A derivation of Equation 14 from gradient descent in parameter space can be found in Appendix B.

For each model-dataset pair, the model is trained on the constructed dataset and on a retain dataset obtained by randomly removing 50% of data points from each class of the dataset, after which the actual changes in model outputs and loss due to the removal of data points are evaluated at 10 randomly selected test data points via $f_r^*(\mathbf{x}_t) - f^*(\mathbf{x}_t)$ and $\ell(f_r^*(\mathbf{x}_t), \mathbf{y}_t) - \ell(f^*(\mathbf{x}_t), \mathbf{y}_t)$, where $f_r^*(\mathbf{x}_t)$ and $f^*(\mathbf{x}_t)$ denote the outputs of the retrained and original infinitely wide neural networks at test data point \mathbf{x}_t after training and are computed by $\mathbf{K}^{\infty}(\mathbf{x}_t, \mathbf{X}_r) \alpha_r^* + f^{(0)}(\mathbf{x}_t)$ and $\mathbf{K}^{\infty}(\mathbf{x}_t, \mathbf{X}) \alpha^* + f^{(0)}(\mathbf{x}_t)$ with $\alpha_r^* := -\frac{1}{\lambda} \nabla_{f_r^*(\mathbf{X}_r)} \hat{\mathcal{L}}_{\mathcal{D}_r}$ and $\alpha^* := -\frac{1}{\lambda} \nabla_{f^*(\mathbf{X})} \hat{\mathcal{L}}_{\mathcal{D}}$. The estimated changes in model outputs and loss are obtained by solving linear system 12, and evaluating $\mathbf{K}_t \Delta \alpha_r^*$ and Equation 9 at the test data points. A comparison of the actual and estimated differences in model outputs and loss is summarized in Figure 4, where, for the outputs of infinitely wide FCNN, all 10 output dimensions are shown. It can be seen that the estimates provided by $\Delta\alpha$ -space method are accurate for both infinitely wide neural networks.

³ \mathbf{K}^{∞} can be written as $\Sigma^{\infty} \otimes \mathbf{I}_{d_{\text{out}}}$ for some $\Sigma^{\infty} \in \mathbb{R}^{|\mathcal{D}| \times |\mathcal{D}|}$ when the infinitely wide neural network uses a fully connected output layer [7]. This can significantly reduce storage space for \mathbf{K}^{∞} and the computation burden for evaluating expressions involving \mathbf{K}^{∞} .

5 Related Work

Our work builds on the work of Koh and Liang [1], who applied influence functions from robust statistics to machine learning to study the effect of perturbing a training data point on model parameters, loss, and outputs. In their work, they identified the scalability issue of influence functions, namely the evaluation of the IHVP becomes computationally expensive as dataset size and model size increase, and consequently proposed to use a stochastic estimation method to approximate these quantities. However, Basu et al. [14] later observed that the stochastic estimation of the IHVP can make influence estimates unreliable in deep learning settings. Several later works focus on improving the scalability of influence functions in θ -space by developing more efficient methods for approximating the IHVP. For example, Schioppa et al. [15] scale up influence functions by using Arnoldi iteration to approximate the IHVP, and demonstrate applicability to vision transformers with up to 300 million parameters, while Grosse et al. [16] employ the Eigenvalue-corrected Kronecker-Factored Approximate Curvature (EK-FAC) to approximate the IHVP, extending influence functions to large language models with up to 52 billion parameters.

Owing to its ability to predict the influence of perturbing training data points on model parameters, influence functions have been widely used for machine unlearning. In particular, influence functions are used by Guo et al. [3] to achieve certified data removal, which guarantees that the unlearned model produced by their method is indistinguishable from one that was never trained on the removed data points, and Warnecke et al. [17] further apply influence functions to enable the unlearning of features and labels by treating feature and label changes as perturbations to training data points.

Linearizable models have also been studied in the literature. Motivated by the works of Du et al. [18] and Allen-Zhu et al. [19], which study the convergence of gradient descent to global minima in overparameterized neural networks and prove that such networks can rapidly drive the training loss to zero while remaining close to their initialization throughout training, Lee et al. [5] investigate the linearizability of such models. In particular, they show that, in the infinite width limit, the training dynamics of deep FCNNs trained by full batch gradient descent on mean squared loss coincide exactly with those of their linearizations, and further demonstrate empirically that this approximation remains accurate in finite width settings, across various model architectures, optimizers, and loss functions, when model size is large relative to dataset size.

6 Conclusion

We presented a dual representation of the influence functions whose computational complexity scales with dataset size rather than model size. We showed analytically that this representation allows the influence of removing data points on parameters to be computed more efficiently than the original representation when the number of model parameters is large relative to the product of model output dimension and retain dataset size. Furthermore, the dual representation also makes it possible to analyze the influence on model outputs and loss in the limit where the number of model parameters goes to infinity. Experimental results obtained by comparing the dual and original representations of influence functions on different machine unlearning tasks further confirmed the computational advantages of the dual representation in settings where working directly in parameter space is difficult or infeasible. Nonetheless, the limitations of the dual representation are that it is applicable only to linearizable models and requires the computation and storage of the NTK matrix, making the usage of this representation expensive for datasets with a large number of data points and classes.

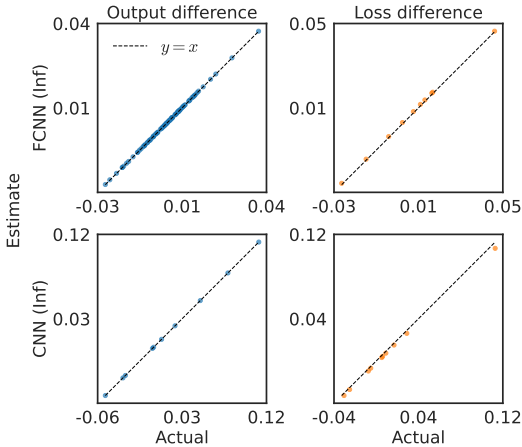


Figure 4: **Comparison of estimated and actual changes in the outputs and loss of two infinitely wide neural networks at 10 test data points after removing 50% of data points from \mathcal{D} .**

References

- [1] Pang Wei Koh and Percy Liang. Understanding black-box predictions via influence functions. In *International Conference on Machine Learning (ICML)*, 2017.
- [2] Thanh Tam Nguyen, Thanh Trung Huynh, Zhao Ren, Phi Le Nguyen, Alan Wee-Chung Liew, Hongzhi Yin, and Quoc Viet Hung Nguyen. A survey of machine unlearning. *ACM Transactions on Intelligent Systems and Technology*, 2025.
- [3] Chuan Guo, Tom Goldstein, Awni Hannun, and Laurens Van Der Maaten. Certified data removal from machine learning models. In *International Conference on Machine Learning (ICML)*, 2020.
- [4] Arthur Jacot, Franck Gabriel, and Clément Hongler. Neural tangent kernel: Convergence and generalization in neural networks. In *Advances in Neural Information Processing Systems (NeurIPS)*, 2018.
- [5] Jaehoon Lee, Lechao Xiao, Samuel Schoenholz, Yasaman Bahri, Roman Novak, Jascha Sohl-Dickstein, and Jeffrey Pennington. Wide neural networks of any depth evolve as linear models under gradient descent. In *Advances in Neural Information Processing Systems (NeurIPS)*, 2019.
- [6] James Bradbury, Roy Frostig, Peter Hawkins, Matthew James Johnson, Chris Leary, Dougal Maclaurin, George Necula, Adam Paszke, Jake VanderPlas, Skye Wanderman-Milne, and Qiao Zhang. JAX: composable transformations of Python+NumPy programs, 2018. URL <http://github.com/google/jax>.
- [7] Roman Novak, Lechao Xiao, Jiri Hron, Jaehoon Lee, Alexander A. Alemi, Jascha Sohl-Dickstein, and Samuel S. Schoenholz. Neural tangents: Fast and easy infinite neural networks in python. In *International Conference on Learning Representations (ICLR)*, 2020. URL <https://github.com/google/neural-tangents>.
- [8] Roman Novak, Jascha Sohl-Dickstein, and Samuel S. Schoenholz. Fast finite width neural tangent kernel. In *International Conference on Machine Learning (ICML)*, 2022.
- [9] Jiri Hron, Yasaman Bahri, Jascha Sohl-Dickstein, and Roman Novak. Infinite attention: Nngp and ntk for deep attention networks. In *International Conference on Machine Learning (ICML)*, 2020.
- [10] Jascha Sohl-Dickstein, Roman Novak, Samuel S Schoenholz, and Jaehoon Lee. On the infinite width limit of neural networks with a standard parameterization. *arXiv preprint*, 2020.
- [11] Insu Han, Amir Zandieh, Jaehoon Lee, Roman Novak, Lechao Xiao, and Amin Karbasi. Fast neural kernel embeddings for general activations. In *Advances in Neural Information Processing Systems (NeurIPS)*, 2022.
- [12] Yann LeCun, Léon Bottou, Yoshua Bengio, and Patrick Haffner. Gradient-based learning applied to document recognition. *Proceedings of the IEEE*, 2002.
- [13] Alex Krizhevsky and Geoffrey Hinton. Learning multiple layers of features from tiny images. 2009.
- [14] S Basu, P Pope, and S Feizi. Influence functions in deep learning are fragile. In *International Conference on Learning Representations (ICLR)*, 2021.
- [15] Andrea Schioppa, Polina Zablotskaia, David Vilar, and Artem Sokolov. Scaling up influence functions. In *AAAI Conference on Artificial Intelligence*, 2022.
- [16] Roger Grosse, Juhan Bae, Cem Anil, Nelson Elhage, Alex Tamkin, Amirhossein Tajdini, Benoit Steiner, Dustin Li, Esin Durmus, Ethan Perez, et al. Studying large language model generalization with influence functions. *arXiv preprint*, 2023.
- [17] Alexander Warnecke, Lukas Pirch, Christian Wressnegger, and Konrad Rieck. Machine unlearning of features and labels. In *Network and Distributed System Security (NDSS) Symposium*, 2023.
- [18] Simon Du, Jason Lee, Haochuan Li, Liwei Wang, and Xiyu Zhai. Gradient descent finds global minima of deep neural networks. In *International Conference on Machine Learning (ICML)*, 2019.
- [19] Zeyuan Allen-Zhu, Yuanzhi Li, and Zhao Song. A convergence theory for deep learning via over-parameterization. In *International Conference on Machine Learning (ICML)*, 2019.

A Proofs

We present proofs for the propositions stated in Section 3.1. The proofs for the setting in which $\|\boldsymbol{\theta} - \boldsymbol{\theta}'\|_2^2$ is replaced by $\|\boldsymbol{\theta}\|_2^2$ are analogous.

Proof of Proposition 3.1. Since $\hat{\boldsymbol{\theta}}^*$ and $\hat{\boldsymbol{\theta}}_r^*$ are the minimizers of $\arg \min_{\boldsymbol{\theta} \in \mathbb{R}^{d_\theta}} \hat{\mathcal{L}}_{\mathcal{D}}(\boldsymbol{\theta})$ and $\arg \min_{\boldsymbol{\theta} \in \mathbb{R}^{d_\theta}} \hat{\mathcal{L}}_{\mathcal{D}_r}(\boldsymbol{\theta})$, respectively, by first-order necessary condition for optimality, they must satisfy

$$\begin{aligned} 0 &= \nabla_{\boldsymbol{\theta}} \hat{\mathcal{L}}_{\mathcal{D}}(\hat{\boldsymbol{\theta}}^*) = \nabla_{\boldsymbol{\theta}} f(\mathbf{X}, \boldsymbol{\theta}')^\top \nabla_{f^{\text{lin}}(\mathbf{X}, \hat{\boldsymbol{\theta}}^*)} \hat{\mathcal{L}}_{\mathcal{D}} + \lambda(\hat{\boldsymbol{\theta}}^* - \boldsymbol{\theta}') \\ 0 &= \nabla_{\boldsymbol{\theta}} \hat{\mathcal{L}}_{\mathcal{D}_r}(\hat{\boldsymbol{\theta}}_r^*) = \nabla_{\boldsymbol{\theta}} f(\mathbf{X}_r, \boldsymbol{\theta}')^\top \nabla_{f^{\text{lin}}(\mathbf{X}_r, \hat{\boldsymbol{\theta}}_r^*)} \hat{\mathcal{L}}_{\mathcal{D}_r} + \lambda(\hat{\boldsymbol{\theta}}_r^* - \boldsymbol{\theta}'), \end{aligned}$$

where $\nabla_{\boldsymbol{\theta}} f(\mathbf{X}, \boldsymbol{\theta}') \in \mathbb{R}^{d_{\text{out}}|\mathcal{D}| \times d_\theta}$ and $\nabla_{f^{\text{lin}}(\mathbf{X}, \hat{\boldsymbol{\theta}}^*)} \hat{\mathcal{L}}_{\mathcal{D}} \in \mathbb{R}^{d_{\text{out}}|\mathcal{D}|}$ are defined as

$$\nabla_{\boldsymbol{\theta}} f(\mathbf{X}, \boldsymbol{\theta}') := \begin{bmatrix} \nabla_{\boldsymbol{\theta}} f(\mathbf{x}^{(1)}, \boldsymbol{\theta}') \\ \vdots \\ \nabla_{\boldsymbol{\theta}} f(\mathbf{x}^{(|\mathcal{D}|)}, \boldsymbol{\theta}') \end{bmatrix} \quad \nabla_{f^{\text{lin}}(\mathbf{X}, \hat{\boldsymbol{\theta}}^*)} \hat{\mathcal{L}}_{\mathcal{D}} := \frac{1}{|\mathcal{D}|} \begin{bmatrix} \nabla_f \ell(f^{\text{lin}}(\mathbf{x}^{(1)}, \hat{\boldsymbol{\theta}}^*), \mathbf{y}^{(1)}) \\ \vdots \\ \nabla_f \ell(f^{\text{lin}}(\mathbf{x}^{(|\mathcal{D}|)}, \hat{\boldsymbol{\theta}}^*), \mathbf{y}^{(|\mathcal{D}|)}) \end{bmatrix},$$

and $\nabla_{\boldsymbol{\theta}} f(\mathbf{X}_r, \boldsymbol{\theta}')$ and $\nabla_{f^{\text{lin}}(\mathbf{X}_r, \hat{\boldsymbol{\theta}}_r^*)} \hat{\mathcal{L}}_{\mathcal{D}_r}$ are defined in the same way. Rearranging terms yields

$$\begin{aligned} \hat{\boldsymbol{\theta}}^* &= \nabla_{\boldsymbol{\theta}} f(\mathbf{X}, \boldsymbol{\theta}')^\top \boldsymbol{\alpha}^* + \boldsymbol{\theta}' \\ \hat{\boldsymbol{\theta}}_r^* &= \nabla_{\boldsymbol{\theta}} f(\mathbf{X}_r, \boldsymbol{\theta}')^\top \boldsymbol{\alpha}_r^* + \boldsymbol{\theta}', \end{aligned}$$

where $\boldsymbol{\alpha}^* := -\frac{1}{\lambda} \nabla_{f^{\text{lin}}(\mathbf{X}, \hat{\boldsymbol{\theta}}^*)} \hat{\mathcal{L}}_{\mathcal{D}} \in \mathbb{R}^{d_{\text{out}}|\mathcal{D}|}$ and $\boldsymbol{\alpha}_r^* := -\frac{1}{\lambda} \nabla_{f^{\text{lin}}(\mathbf{X}_r, \hat{\boldsymbol{\theta}}_r^*)} \hat{\mathcal{L}}_{\mathcal{D}_r} \in \mathbb{R}^{d_{\text{out}}|\mathcal{D}_r|}$. Assume, without loss of generality, that data points in \mathcal{D}_f are the first $|\mathcal{D}_f|$ data points in \mathcal{D} , then by defining $\tilde{\boldsymbol{\alpha}}_r^* := [\mathbf{0}^\top, \boldsymbol{\alpha}_r^{*\top}]^\top \in \mathbb{R}^{d_{\text{out}}|\mathcal{D}|}$, $\hat{\boldsymbol{\theta}}_r^*$ can be rewritten as $\hat{\boldsymbol{\theta}}_r^* = \nabla_{\boldsymbol{\theta}} f(\mathbf{X}, \boldsymbol{\theta}')^\top \tilde{\boldsymbol{\alpha}}_r^* + \boldsymbol{\theta}'$. Subtracting $\hat{\boldsymbol{\theta}}^*$ from $\hat{\boldsymbol{\theta}}_r^*$ yields

$$\hat{\boldsymbol{\theta}}_r^* - \hat{\boldsymbol{\theta}}^* = \nabla_{\boldsymbol{\theta}} f(\mathbf{X}, \boldsymbol{\theta}')^\top \Delta \boldsymbol{\alpha}_r^*,$$

where

$$\Delta \boldsymbol{\alpha}_r^* = \tilde{\boldsymbol{\alpha}}_r^* - \boldsymbol{\alpha}^* = \begin{bmatrix} \frac{1}{\lambda} \nabla_{f^{\text{lin}}(\mathbf{X}_f, \hat{\boldsymbol{\theta}}^*)} \hat{\mathcal{L}}_{\mathcal{D}} \\ -\frac{1}{\lambda} \left(\nabla_{f^{\text{lin}}(\mathbf{X}_r, \hat{\boldsymbol{\theta}}_r^*)} \hat{\mathcal{L}}_{\mathcal{D}_r} - \nabla_{f^{\text{lin}}(\mathbf{X}_r, \hat{\boldsymbol{\theta}}^*)} \hat{\mathcal{L}}_{\mathcal{D}} \right) \end{bmatrix}.$$

□

Proof of Proposition 3.2. By definition of minimizer and the fact that $\mathcal{C} \subset \mathbb{R}^{d_\theta}$, we know $\hat{\boldsymbol{\theta}}_r^* := \arg \min_{\boldsymbol{\theta} \in \mathbb{R}^{d_\theta}} \hat{\mathcal{L}}_{\mathcal{D}_r}(\boldsymbol{\theta})$ and $\hat{\boldsymbol{\theta}}_{r,c}^* := \arg \min_{\boldsymbol{\theta} \in \mathcal{C}} \hat{\mathcal{L}}_{\mathcal{D}_r}(\boldsymbol{\theta})$ satisfy

$$\begin{aligned} \hat{\mathcal{L}}_{\mathcal{D}_r}(\hat{\boldsymbol{\theta}}_r^*) &\leq \hat{\mathcal{L}}_{\mathcal{D}_r}(\boldsymbol{\theta}), \quad \forall \boldsymbol{\theta} \in \mathcal{C} \\ \hat{\mathcal{L}}_{\mathcal{D}_r}(\hat{\boldsymbol{\theta}}_{r,c}^*) &\leq \hat{\mathcal{L}}_{\mathcal{D}_r}(\boldsymbol{\theta}), \quad \forall \boldsymbol{\theta} \in \mathcal{C}. \end{aligned}$$

Thus, $\hat{\boldsymbol{\theta}}_r^*$ and $\hat{\boldsymbol{\theta}}_{r,c}^*$ are both minimizers of $\arg \min_{\boldsymbol{\theta} \in \mathcal{C}} \hat{\mathcal{L}}_{\mathcal{D}_r}(\boldsymbol{\theta})$. When ℓ is convex with respect to the model output, $\arg \min_{\boldsymbol{\theta} \in \mathcal{C}} \hat{\mathcal{L}}_{\mathcal{D}_r}(\boldsymbol{\theta})$ is a convex optimization problem with a strictly convex objective function. As a result, the global minimizer is unique, and hence $\hat{\boldsymbol{\theta}}_r^* = \hat{\boldsymbol{\theta}}_{r,c}^*$. □

Proof of Proposition 3.3. When ℓ is convex with respect to the model output and $\lambda > 0$, both $\arg \min_{\Delta \boldsymbol{\alpha} \in \mathbb{R}^{d_{\text{out}}|\mathcal{D}|}} \tilde{\mathcal{L}}_{\mathcal{D}_r}(\Delta \boldsymbol{\alpha})$ and $\arg \min_{\boldsymbol{\theta} \in \mathcal{C}} \hat{\mathcal{L}}_{\mathcal{D}_r}(\boldsymbol{\theta})$ are convex optimization problems with strictly convex objective functions. As a result, their minimizers $\Delta \boldsymbol{\alpha}_r^*$ and $\hat{\boldsymbol{\theta}}_{r,c}^*$ are unique. If $\nabla_{\boldsymbol{\theta}} f(\mathbf{X}, \boldsymbol{\theta}')$ has full row rank, then $\phi(\cdot)$ is injective and for every $\boldsymbol{\theta} \in \text{Im}(\phi)$ there exists exactly one $\Delta \boldsymbol{\alpha}$ such that $\phi(\Delta \boldsymbol{\alpha}) = \boldsymbol{\theta}$. Since, by proposition 3.1 and 3.2, we know $\hat{\boldsymbol{\theta}}_{r,c}^* = \phi(\Delta \boldsymbol{\alpha}_r^*)$ and $\hat{\boldsymbol{\theta}}_{r,c}^* \in \text{Im}(\phi)$, we can conclude that $\Delta \boldsymbol{\alpha}_r^* \xrightarrow[\phi^{-1}(\cdot)]{\phi(\cdot)} \hat{\boldsymbol{\theta}}_{r,c}^*$. □

B Derivations

We present detailed derivations for the equations shown in Section 2.1 and 3.2. The derivations for the setting in which $\|\boldsymbol{\theta} - \boldsymbol{\theta}'\|_2^2$ is replaced by $\|\boldsymbol{\theta}\|_2^2$ are analogous.

B.1 Derivation for Equation 1

The following derivation, adapted from [1], serves to introduce our notation and to generalize their single data point removal setting to a multiple data points removal setting.

In the multiple data points removal setting, we define the upweighted empirical risk as $\mathcal{L}_{\mathcal{D}}(\boldsymbol{\theta}, \epsilon) := \mathcal{L}_{\mathcal{D}}(\boldsymbol{\theta}) + |\mathcal{D}_f| \mathcal{L}_{\mathcal{D}_f}(\boldsymbol{\theta}) \epsilon$. Substituting $\mathcal{L}_{\mathcal{D}}(\boldsymbol{\theta})$ and $\mathcal{L}_{\mathcal{D}_f}(\boldsymbol{\theta})$ with their respective definitions and setting $\epsilon = -\frac{1}{|\mathcal{D}|}$ yields $\mathcal{L}_{\mathcal{D}}(\boldsymbol{\theta}, -\frac{1}{|\mathcal{D}|}) = \frac{|\mathcal{D}_r|}{|\mathcal{D}|} \mathcal{L}_{\mathcal{D}_r}(\boldsymbol{\theta})$. Since $\frac{|\mathcal{D}_r|}{|\mathcal{D}|} > 0$ and $\mathcal{L}_{\mathcal{D}}(\boldsymbol{\theta}, -\frac{1}{|\mathcal{D}|})$ is a scalar multiple of $\mathcal{L}_{\mathcal{D}_r}(\boldsymbol{\theta})$, the two optimization problems $\arg \min_{\boldsymbol{\theta} \in \mathbb{R}^{d_{\boldsymbol{\theta}}}} \mathcal{L}_{\mathcal{D}_r}(\boldsymbol{\theta})$ and $\arg \min_{\boldsymbol{\theta} \in \mathbb{R}^{d_{\boldsymbol{\theta}}}} \mathcal{L}_{\mathcal{D}}(\boldsymbol{\theta}, -\frac{1}{|\mathcal{D}|})$ share the same minimizer, i.e., $\boldsymbol{\theta}_r^* = \boldsymbol{\theta}^*(-\frac{1}{|\mathcal{D}|})$.

By first order necessary condition of optimality, $\boldsymbol{\theta}^*$ and $\boldsymbol{\theta}^*(\epsilon)$ must satisfy $\nabla_{\boldsymbol{\theta}} \mathcal{L}_{\mathcal{D}}(\boldsymbol{\theta}^*) = \mathbf{0}$ and $\nabla_{\boldsymbol{\theta}} \mathcal{L}_{\mathcal{D}}(\boldsymbol{\theta}^*(\epsilon), \epsilon) = \mathbf{0}$, respectively. When ϵ is small, $\boldsymbol{\theta}^*(\epsilon)$ is close to $\boldsymbol{\theta}^*$ and $\nabla_{\boldsymbol{\theta}} \mathcal{L}_{\mathcal{D}}(\boldsymbol{\theta}^*(\epsilon), \epsilon)$ can be accurately approximated by its first-order Taylor expansion around $\boldsymbol{\theta}^*$, so the optimality condition for $\boldsymbol{\theta}^*(\epsilon)$ becomes $\nabla_{\boldsymbol{\theta}} \mathcal{L}_{\mathcal{D}}(\boldsymbol{\theta}^*, \epsilon) + \nabla_{\boldsymbol{\theta}}^2 \mathcal{L}_{\mathcal{D}}(\boldsymbol{\theta}^*, \epsilon) (\boldsymbol{\theta}^*(\epsilon) - \boldsymbol{\theta}^*) \approx \mathbf{0}$. Rearranging terms and taking first- and second-order derivatives of $\mathcal{L}_{\mathcal{D}}(\boldsymbol{\theta}, \epsilon)$ with respect to $\boldsymbol{\theta}$ yields

$$\begin{aligned} \boldsymbol{\theta}^*(\epsilon) &\approx \boldsymbol{\theta}^* - \nabla_{\boldsymbol{\theta}}^2 \mathcal{L}_{\mathcal{D}}(\boldsymbol{\theta}^*, \epsilon)^{-1} \nabla_{\boldsymbol{\theta}} \mathcal{L}_{\mathcal{D}}(\boldsymbol{\theta}^*, \epsilon) \\ &= \boldsymbol{\theta}^* - (\nabla_{\boldsymbol{\theta}}^2 \mathcal{L}_{\mathcal{D}}(\boldsymbol{\theta}^*) + |\mathcal{D}_f| \nabla_{\boldsymbol{\theta}}^2 \mathcal{L}_{\mathcal{D}_f}(\boldsymbol{\theta}^*) \epsilon)^{-1} |\mathcal{D}_f| \nabla_{\boldsymbol{\theta}} \mathcal{L}_{\mathcal{D}_f}(\boldsymbol{\theta}^*) \epsilon. \end{aligned}$$

When $\epsilon = -\frac{1}{|\mathcal{D}|}$, using the relation $\boldsymbol{\theta}_r^* = \boldsymbol{\theta}^*(-\frac{1}{|\mathcal{D}|})$, the above equation becomes $\boldsymbol{\theta}_r^* \approx \boldsymbol{\theta}^* + \frac{|\mathcal{D}_f|}{|\mathcal{D}|} \mathbf{H}_{\boldsymbol{\theta}^*}^{-1} \nabla_{\boldsymbol{\theta}} \mathcal{L}_{\mathcal{D}_f}(\boldsymbol{\theta}^*)$, where $\mathbf{H}_{\boldsymbol{\theta}^*}^{-1} := (\nabla_{\boldsymbol{\theta}}^2 \mathcal{L}_{\mathcal{D}}(\boldsymbol{\theta}^*) - \frac{|\mathcal{D}_f|}{|\mathcal{D}|} \nabla_{\boldsymbol{\theta}}^2 \mathcal{L}_{\mathcal{D}_f}(\boldsymbol{\theta}^*))^{-1}$ can be further approximated by $\nabla_{\boldsymbol{\theta}}^2 \mathcal{L}_{\mathcal{D}}(\boldsymbol{\theta}^*)^{-1}$ when $\frac{|\mathcal{D}_f|}{|\mathcal{D}|}$ is small, due to the identity $(\mathbf{A} + \epsilon \mathbf{X})^{-1} = \mathbf{A}^{-1} - \epsilon \mathbf{A}^{-1} \mathbf{X} \mathbf{A}^{-1} + \mathcal{O}(\epsilon^2)$.

B.2 Derivation for Equation 5

The derivation of Equation 5 is identical to that of Equation 1, with only a few minor tweaks. Specifically, by replacing $\mathcal{L}_{\mathcal{D}}(\boldsymbol{\theta}, \epsilon)$ with $\tilde{\mathcal{L}}_{\mathcal{D}}(\Delta \boldsymbol{\alpha}, \epsilon) := \tilde{\mathcal{L}}_{\mathcal{D}}(\Delta \boldsymbol{\alpha}) + |\mathcal{D}_f| \tilde{\mathcal{L}}_{\mathcal{D}_f}(\Delta \boldsymbol{\alpha}) \epsilon$, but otherwise following the same derivation as in Section B.1, one can show that

$$\Delta \boldsymbol{\alpha}_r^* \approx \Delta \boldsymbol{\alpha}^* + \frac{|\mathcal{D}_f|}{|\mathcal{D}|} \mathbf{H}_{\Delta \boldsymbol{\alpha}^*}^{-1} \nabla_{\Delta \boldsymbol{\alpha}} \tilde{\mathcal{L}}_{\mathcal{D}_f}(\Delta \boldsymbol{\alpha}^*),$$

where $\mathbf{H}_{\Delta \boldsymbol{\alpha}^*}^{-1} := \left(\nabla_{\Delta \boldsymbol{\alpha}}^2 \tilde{\mathcal{L}}_{\mathcal{D}}(\Delta \boldsymbol{\alpha}^*) - \frac{|\mathcal{D}_f|}{|\mathcal{D}|} \nabla_{\Delta \boldsymbol{\alpha}}^2 \tilde{\mathcal{L}}_{\mathcal{D}_f}(\Delta \boldsymbol{\alpha}^*) \right)^{-1}$ can be further approximated by $\nabla_{\Delta \boldsymbol{\alpha}}^2 \tilde{\mathcal{L}}_{\mathcal{D}}(\Delta \boldsymbol{\alpha}^*)^{-1}$ when $\frac{|\mathcal{D}_f|}{|\mathcal{D}|}$ is small. To obtain Equation 5, it remains to show that $\Delta \boldsymbol{\alpha}^* = \mathbf{0}$, which follows from Proposition 3.2 and 3.3. Specifically, these two propositions imply that, $\Delta \boldsymbol{\alpha}^*$, $\hat{\boldsymbol{\theta}}^*$ and $\hat{\boldsymbol{\theta}}_c^* := \arg \min_{\boldsymbol{\theta} \in \mathcal{C}} \hat{\mathcal{L}}_{\mathcal{D}}(\boldsymbol{\theta})$ are related by

$$\Delta \boldsymbol{\alpha}^* \xrightarrow[\phi^{-1}(\cdot)]{\phi(\cdot)} \hat{\boldsymbol{\theta}}_c^* = \hat{\boldsymbol{\theta}}^*.$$

Therefore, $\hat{\boldsymbol{\theta}}^* = \hat{\boldsymbol{\theta}}_c^* + \nabla_{\boldsymbol{\theta}} f(\mathbf{X}, \boldsymbol{\theta}')^{\top} \Delta \boldsymbol{\alpha}^*$ and rearranging terms yields $\nabla_{\boldsymbol{\theta}} f(\mathbf{X}, \boldsymbol{\theta}')^{\top} \Delta \boldsymbol{\alpha}^* = \mathbf{0}$. Since $\nabla_{\boldsymbol{\theta}} f(\mathbf{X}, \boldsymbol{\theta}')$ is assumed to have full row rank, $\nabla_{\boldsymbol{\theta}} f(\mathbf{X}, \boldsymbol{\theta}')^{\top}$ has full column rank and a trivial null space, i.e., $\ker(\nabla_{\boldsymbol{\theta}} f(\mathbf{X}, \boldsymbol{\theta}')^{\top}) = \{\mathbf{0}\}$, which implies that $\Delta \boldsymbol{\alpha}^* = \mathbf{0}$.

B.3 Derivation for Equations 6 and 7

For any dataset \mathcal{D}_i , by definition of $\tilde{\mathcal{L}}_{\mathcal{D}_i}(\Delta \boldsymbol{\alpha})$, $\nabla_{\Delta \boldsymbol{\alpha}} \tilde{\mathcal{L}}_{\mathcal{D}_i}(\Delta \boldsymbol{\alpha})$ and $\nabla_{\Delta \boldsymbol{\alpha}}^2 \tilde{\mathcal{L}}_{\mathcal{D}_i}(\Delta \boldsymbol{\alpha})$ are given by

$$\nabla_{\Delta \boldsymbol{\alpha}} \tilde{\mathcal{L}}_{\mathcal{D}_i}(\Delta \boldsymbol{\alpha}) = \mathbf{K}(\mathbf{X}, \mathbf{X}_i) \nabla_{g^{\text{in}}(\mathbf{X}_i, \Delta \boldsymbol{\alpha})} \tilde{\mathcal{L}}_{\mathcal{D}_i} + \lambda \nabla_{\boldsymbol{\theta}} f(\mathbf{X}, \boldsymbol{\theta}') (\hat{\boldsymbol{\theta}}^* - \boldsymbol{\theta}') + \lambda \mathbf{K} \Delta \boldsymbol{\alpha} \quad (\text{A.1})$$

$$\nabla_{\Delta \boldsymbol{\alpha}}^2 \tilde{\mathcal{L}}_{\mathcal{D}_i}(\Delta \boldsymbol{\alpha}) = \mathbf{K}(\mathbf{X}, \mathbf{X}_i) \nabla_{g^{\text{in}}(\mathbf{X}_i, \Delta \boldsymbol{\alpha})}^2 \tilde{\mathcal{L}}_{\mathcal{D}_i} \mathbf{K}(\mathbf{X}_i, \mathbf{X}) + \lambda \mathbf{K}, \quad (\text{A.2})$$

where $\mathbf{K}(\mathbf{X}, \mathbf{X}_i) := [\mathbf{K}(\mathbf{X}, \mathbf{x}^{(1)}), \dots, \mathbf{K}(\mathbf{X}, \mathbf{x}^{(|\mathcal{D}_i|)})] \in \mathbb{R}^{d_{\text{out}}|\mathcal{D}| \times d_{\text{out}}|\mathcal{D}_i|}$,

$$\nabla_{g^{\text{lin}}(\mathbf{X}_i, \Delta\alpha)} \tilde{\mathcal{L}}_{\mathcal{D}_i} := \frac{1}{|\mathcal{D}_i|} \begin{bmatrix} \nabla_f \ell(g^{\text{lin}}(\mathbf{x}^{(1)}, \Delta\alpha), \mathbf{y}^{(1)}) \\ \vdots \\ \nabla_f \ell(g^{\text{lin}}(\mathbf{x}^{(|\mathcal{D}_i|)}, \Delta\alpha), \mathbf{y}^{(|\mathcal{D}_i|)}) \end{bmatrix} \in \mathbb{R}^{d_{\text{out}}|\mathcal{D}_i|}.$$

and $\nabla_{g^{\text{lin}}(\mathbf{X}_i, \Delta\alpha)}^2 \tilde{\mathcal{L}}_{\mathcal{D}_i} \in \mathbb{R}^{d_{\text{out}}|\mathcal{D}_i| \times d_{\text{out}}|\mathcal{D}_i|}$ is a block diagonal matrix whose blocks are

$$\frac{1}{|\mathcal{D}_i|} \nabla_f^2 \ell(g^{\text{lin}}(\mathbf{x}, \Delta\alpha), \mathbf{y}) \in \mathbb{R}^{d_{\text{out}} \times d_{\text{out}}}, \forall (\mathbf{x}, \mathbf{y}) \in \mathcal{D}_i.$$

$\nabla_{\Delta\alpha} \tilde{\mathcal{L}}_{\mathcal{D}_f}(\Delta\alpha)$, $\nabla_{\Delta\alpha}^2 \tilde{\mathcal{L}}_{\mathcal{D}_f}(\Delta\alpha)$ and $\nabla_{\Delta\alpha}^2 \tilde{\mathcal{L}}_{\mathcal{D}}(\Delta\alpha)$ are obtained by replacing \mathcal{D}_i in Equations A.1 and A.2 with \mathcal{D}_f and \mathcal{D} .

Equation 7 is obtained by evaluating $\nabla_{\Delta\alpha} \tilde{\mathcal{L}}_{\mathcal{D}_f}(\Delta\alpha)$ at $\Delta\alpha^* = \mathbf{0}$,

$$\begin{aligned} \nabla_{\Delta\alpha} \tilde{\mathcal{L}}_{\mathcal{D}_f}(\mathbf{0}) &= \mathbf{K}(\mathbf{X}, \mathbf{X}_f) \nabla_{g^{\text{lin}}(\mathbf{X}_f, \mathbf{0})} \tilde{\mathcal{L}}_{\mathcal{D}_f} + \lambda \nabla_{\theta} f(\mathbf{X}, \theta') (\hat{\theta}^* - \theta') \\ &= \mathbf{K}(\mathbf{X}_f, \mathbf{X})^\top \nabla_{f^{\text{lin}}(\mathbf{X}_f, \hat{\theta}^*)} \hat{\mathcal{L}}_{\mathcal{D}_f} + \lambda \mathbf{K} \alpha^*, \end{aligned}$$

where we have used the fact that $\hat{\theta}^* - \theta' = \nabla_{\theta} f(\mathbf{X}, \theta')^\top \alpha^*$ and $g^{\text{lin}}(\cdot, \mathbf{0}) = f^{\text{lin}}(\cdot, \hat{\theta}^*)$. By definition of $\mathbf{H}_{\Delta\alpha}$, we have

$$\begin{aligned} \mathbf{H}_{\Delta\alpha} &= \nabla_{\Delta\alpha}^2 \tilde{\mathcal{L}}_{\mathcal{D}}(\Delta\alpha) - \frac{|\mathcal{D}_f|}{|\mathcal{D}|} \nabla_{\Delta\alpha}^2 \tilde{\mathcal{L}}_{\mathcal{D}_f}(\Delta\alpha) \\ &= \frac{|\mathcal{D}_r|}{|\mathcal{D}|} \left(\mathbf{K}(\mathbf{X}_r, \mathbf{X})^\top \nabla_{g^{\text{lin}}(\mathbf{X}_r, \Delta\alpha)}^2 \tilde{\mathcal{L}}_{\mathcal{D}_r} \mathbf{K}(\mathbf{X}_r, \mathbf{X}) + \lambda \mathbf{K} \right), \end{aligned}$$

evaluating $\mathbf{H}_{\Delta\alpha}$ at $\Delta\alpha^* = \mathbf{0}$ and using the equality $g^{\text{lin}}(\cdot, \mathbf{0}) = f^{\text{lin}}(\cdot, \hat{\theta}^*)$ gives Equation 6.

B.4 Derivation for Equations 8 and 9

The first-order Taylor expansion of $g^{\text{lin}}(\mathbf{x}_t, \Delta\alpha_r^*)$ and $\tilde{\mathcal{L}}_{\{\mathbf{z}_t\}}(\Delta\alpha_r^*)$ around $\Delta\alpha^* = \mathbf{0}$ gives

$$\begin{aligned} g^{\text{lin}}(\mathbf{x}_t, \Delta\alpha_r^*) - g^{\text{lin}}(\mathbf{x}_t, \mathbf{0}) &= \mathbf{K}(\mathbf{x}_t, \mathbf{X}) \Delta\alpha_r^* \\ \tilde{\mathcal{L}}_{\{\mathbf{z}_t\}}(\Delta\alpha_r^*) - \tilde{\mathcal{L}}_{\{\mathbf{z}_t\}}(\mathbf{0}) &\approx \nabla_{\Delta\alpha} \tilde{\mathcal{L}}_{\{\mathbf{z}_t\}}(\mathbf{0})^\top \Delta\alpha_r^*. \end{aligned}$$

When $g^{\text{lin}}(\mathbf{x}_t, \Delta\alpha)$ and $\tilde{\mathcal{L}}_{\{\mathbf{z}_t\}}(\Delta\alpha)$ are evaluated at $\mathbf{0}$, by their definitions, we have $g^{\text{lin}}(\mathbf{x}_t, \mathbf{0}) = f^{\text{lin}}(\mathbf{x}_t, \hat{\theta}^*)$ and

$$\tilde{\mathcal{L}}_{\{\mathbf{z}_t\}}(\mathbf{0}) = \ell(f^{\text{lin}}(\mathbf{x}_t, \hat{\theta}^*), \mathbf{y}_t) + \frac{\lambda}{2} \|\hat{\theta}^* - \theta'\|_2^2 = \hat{\mathcal{L}}_{\{\mathbf{z}_t\}}(\hat{\theta}^*).$$

When they are evaluated at $\Delta\alpha_r^*$, by Proposition 3.1 and definition of $f^{\text{lin}}(\cdot, \theta)$, we have

$$\begin{aligned} g^{\text{lin}}(\mathbf{x}_t, \Delta\alpha_r^*) &= f^{\text{lin}}(\mathbf{x}_t, \hat{\theta}^*) + \mathbf{K}(\mathbf{x}_t, \mathbf{X}) (\tilde{\alpha}_r^* - \alpha^*) \\ &= f^{\text{lin}}(\mathbf{x}_t, \hat{\theta}^*) + \nabla_{\theta} f(\mathbf{x}_t, \theta') (\hat{\theta}_r^* - \theta') - \nabla_{\theta} f(\mathbf{x}_t, \theta') (\hat{\theta}^* - \theta') \\ &= f(\mathbf{x}_t, \theta') + \nabla_{\theta} f(\mathbf{x}_t, \theta') (\hat{\theta}_r^* - \theta') \\ &= f^{\text{lin}}(\mathbf{x}_t, \hat{\theta}_r^*), \end{aligned}$$

and

$$\begin{aligned} \tilde{\mathcal{L}}_{\{\mathbf{z}_t\}}(\Delta\alpha_r^*) &= \ell(f^{\text{lin}}(\mathbf{x}_t, \hat{\theta}_r^*), \mathbf{y}_t) + \frac{\lambda}{2} \|\hat{\theta}^* + \nabla_{\theta} f(\mathbf{X}, \theta')^\top \Delta\alpha_r^* - \theta'\|_2^2 \\ &= \ell(f^{\text{lin}}(\mathbf{x}_t, \hat{\theta}_r^*), \mathbf{y}_t) + \frac{\lambda}{2} \|\hat{\theta}_r^* - \theta'\|_2^2 \\ &= \hat{\mathcal{L}}_{\{\mathbf{z}_t\}}(\hat{\theta}_r^*). \end{aligned}$$

Combining these results gives Equations 8 and 9.

B.5 Derivation for Equation 13

Evaluating Equation 9 at all data points in \mathcal{D}_t is equivalent to performing the matrix vector product:

$$\begin{bmatrix} \left(\mathbf{K}(\mathbf{x}_t^{(1)}, \mathbf{X})^\top \nabla_{f^{\text{lin}}(\mathbf{x}_t^{(1)}, \hat{\boldsymbol{\theta}}^*)} \hat{\mathcal{L}}_{\{\mathbf{z}_t^{(1)}\}} + \lambda \mathbf{K} \boldsymbol{\alpha}^* \right)^\top \\ \vdots \\ \left(\mathbf{K}(\mathbf{x}_t^{(|\mathcal{D}_t|)}, \mathbf{X})^\top \nabla_{f^{\text{lin}}(\mathbf{x}_t^{(|\mathcal{D}_t|)}, \hat{\boldsymbol{\theta}}^*)} \hat{\mathcal{L}}_{\{\mathbf{z}_t^{(|\mathcal{D}_t|)}\}} + \lambda \mathbf{K} \boldsymbol{\alpha}^* \right)^\top \end{bmatrix} \Delta \boldsymbol{\alpha}_r^*.$$

Assume f^{lin} has scalar-valued output, the above product can be rewritten as

$$\begin{bmatrix} \nabla_{f^{\text{lin}}(\mathbf{x}_t^{(1)}, \hat{\boldsymbol{\theta}}^*)} \hat{\mathcal{L}}_{\{\mathbf{z}_t^{(1)}\}} \\ \vdots \\ \nabla_{f^{\text{lin}}(\mathbf{x}_t^{(|\mathcal{D}_t|)}, \hat{\boldsymbol{\theta}}^*)} \hat{\mathcal{L}}_{\{\mathbf{z}_t^{(|\mathcal{D}_t|)}\}} \end{bmatrix} \odot \left(\begin{bmatrix} \mathbf{K}(\mathbf{x}_t^{(1)}, \mathbf{X}) \\ \vdots \\ \mathbf{K}(\mathbf{x}_t^{(|\mathcal{D}_t|)}, \mathbf{X}) \end{bmatrix} \Delta \boldsymbol{\alpha}_r^* \right) + \lambda \begin{bmatrix} \boldsymbol{\alpha}^{*\top} \mathbf{K} \Delta \boldsymbol{\alpha}_r^* \\ \vdots \\ \boldsymbol{\alpha}^{*\top} \mathbf{K} \Delta \boldsymbol{\alpha}_r^* \end{bmatrix},$$

which gives Equation 13. The generalization to vector-valued f^{lin} follows by noticing

$$\mathbf{1}^\top \left(\nabla_{f^{\text{lin}}(\mathbf{x}_t, \hat{\boldsymbol{\theta}}^*)} \hat{\mathcal{L}}_{\{\mathbf{z}_t\}} \odot (\mathbf{K}(\mathbf{x}_t, \mathbf{X}) \Delta \boldsymbol{\alpha}_r^*) \right) = \nabla_{f^{\text{lin}}(\mathbf{x}_t, \hat{\boldsymbol{\theta}}^*)} \hat{\mathcal{L}}_{\{\mathbf{z}_t\}}^\top \mathbf{K}(\mathbf{x}_t, \mathbf{X}) \Delta \boldsymbol{\alpha}_r^*,$$

where $\mathbf{1} \in \mathbb{R}^{d_{\text{out}}}$ denotes the all-ones vector.

B.6 Derivation for Equation 14

When full-batch gradient descent (GD) is used to minimize $\hat{\mathcal{L}}_{\mathcal{D}}(\boldsymbol{\theta})$ with $\boldsymbol{\theta}'$ set to the initial parameters $\boldsymbol{\theta}^{(0)}$, the GD update rule for $\boldsymbol{\theta}$ can be written as

$$\boldsymbol{\theta}^{(k+1)} = \boldsymbol{\theta}^{(k)} - \eta \cdot \left(\nabla_{\boldsymbol{\theta}} f(\mathbf{X}, \boldsymbol{\theta}^{(0)})^\top \nabla_{f^{\text{lin}}(\mathbf{X}, \boldsymbol{\theta}^{(k)})} \hat{\mathcal{L}}_{\mathcal{D}} + \lambda \cdot (\boldsymbol{\theta}^{(k)} - \boldsymbol{\theta}^{(0)}) \right). \quad (\text{A.3})$$

By definition of $f^{\text{lin}}(\cdot, \boldsymbol{\theta})$ and Equation A.3, the difference in the model output at any data point \mathbf{x} , between any two consecutive GD iterations, is given by

$$\begin{aligned} & f^{\text{lin}}(\mathbf{x}, \boldsymbol{\theta}^{(k+1)}) - f^{\text{lin}}(\mathbf{x}, \boldsymbol{\theta}^{(k)}) \\ &= -\eta \cdot \left(\nabla_{\boldsymbol{\theta}} f(\mathbf{x}, \boldsymbol{\theta}^{(0)}) \nabla_{\boldsymbol{\theta}} f(\mathbf{X}, \boldsymbol{\theta}^{(0)})^\top \nabla_{f^{\text{lin}}(\mathbf{X}, \boldsymbol{\theta}^{(k)})} \hat{\mathcal{L}}_{\mathcal{D}} + \lambda \cdot \nabla_{\boldsymbol{\theta}} f(\mathbf{x}, \boldsymbol{\theta}^{(0)}) (\boldsymbol{\theta} - \boldsymbol{\theta}^{(0)}) \right) \\ &= -\eta \cdot \left(\mathbf{K}(\mathbf{x}, \mathbf{X}) \nabla_{f^{\text{lin}}(\mathbf{X}, \boldsymbol{\theta}^{(k)})} \hat{\mathcal{L}}_{\mathcal{D}} + \lambda \cdot (f^{\text{lin}}(\mathbf{x}, \boldsymbol{\theta}^{(k)}) - f^{\text{lin}}(\mathbf{x}, \boldsymbol{\theta}^{(0)})) \right). \end{aligned} \quad (\text{A.4})$$

Evaluating Equation A.4 on all data points in \mathcal{D} and taking the limit $d_{\boldsymbol{\theta}} \rightarrow \infty$ yields Equation 14. In addition, Equation 14 can be obtained more rigorously by deriving the functional gradient of

$$\hat{\mathcal{L}}_{\mathcal{D}}[\Delta f] := \frac{1}{|\mathcal{D}|} \sum_{(\mathbf{x}, \mathbf{y}) \in \mathcal{D}} \left(\ell(f_0(\mathbf{x}) + \Delta f(\mathbf{x}), \mathbf{y}) + \frac{\lambda}{2} \|\Delta f\|_{\mathcal{H}}^2 \right)$$

with respect to $\Delta f(\cdot) := f(\cdot) - f_0(\cdot)$, where \mathcal{H} denotes the reproducing kernel Hilbert space (RKHS) induced by $\mathbf{K}^\infty(\cdot, \cdot)$. Specifically,

$$\begin{aligned} \frac{\delta \hat{\mathcal{L}}_{\mathcal{D}}}{\delta \Delta f} &= \frac{1}{|\mathcal{D}|} \sum_{(\mathbf{x}, \mathbf{y}) \in \mathcal{D}} \left(\frac{\delta \ell(f_0(\mathbf{x}) + \Delta f(\mathbf{x}), \mathbf{y})}{\delta \Delta f} + \frac{\lambda}{2} \frac{\delta \|\Delta f\|_{\mathcal{H}}^2}{\delta \Delta f} \right) \\ &= \frac{1}{|\mathcal{D}|} \sum_{(\mathbf{x}, \mathbf{y}) \in \mathcal{D}} \left(\mathbf{K}^\infty(\cdot, \mathbf{x}) \nabla_f \ell(f(\mathbf{x}), \mathbf{y}) + \lambda \Delta f \right) \\ &= \frac{1}{|\mathcal{D}|} \cdot \mathbf{K}^\infty(\cdot, \mathbf{X}) \nabla_f \ell(f(\mathbf{X}), \mathbf{Y}) + \lambda (f(\cdot) - f_0(\cdot)) \end{aligned} \quad (\text{A.5})$$

where we have used $\frac{\delta \Delta f(\mathbf{x})}{\delta \Delta f} = \mathbf{K}^\infty(\cdot, \mathbf{x})$ and $\nabla_f \ell(f(\mathbf{X}), \mathbf{Y})$ is defined as

$$\nabla_f \ell(f(\mathbf{X}), \mathbf{Y}) := \begin{bmatrix} \nabla_f \ell(f(\mathbf{x}^{(1)}), \mathbf{y}^{(1)}) \\ \vdots \\ \nabla_f \ell(f(\mathbf{x}^{(|\mathcal{D}|)}), \mathbf{y}^{(|\mathcal{D}|)}) \end{bmatrix} \in \mathbb{R}^{d_{\text{out}} |\mathcal{D}|}.$$

Multiplying Equation A.5 by $-\eta$ gives the update direction for the KGD, and evaluating it at all data points in \mathcal{D} gives Equation 14.